Received: 9 September 2022 | Revised: 27 January 2023 | Accepted: 20 February 2023

DOI: 10.1002/jex2.78

SHORT COMMUNICATION

Removal and identification of external protein corona members from RBC-derived extracellular vesicles by surface manipulating antimicrobial peptides

Priyanka Singh[1,2] | **Imola Cs. Szigyártó**[1] | **Maria Ricci**[1] | **Anikó Gaál**[3] | **Mayra Maritza Quemé-Peña**[1,2] | **Diána Kitka**[2,3] | **Lívia Fülöp**[4] | **Lilla Turiák**[5] | **László Drahos**[5] | **Zoltán Varga**[3] | **Tamás Beke-Somfai**[1]

[1]Institute of Materials and Environmental Chemistry, Biomolecular Self-assembly Research Group, Research Centre for Natural Sciences, Budapest, Hungary

[2]Hevesy György PhD School of Chemistry, ELTE Eötvös Loránd University, Budapest, Hungary

[3]Institute of Materials and Environmental Chemistry, Biological Nanochemistry Research Group, Research Centre for Natural Sciences, Budapest, Hungary

[4]Department of Medical Chemistry, University of Szeged, Szeged, Hungary

[5]Institute of Organic Chemistry, MS Proteomics Research Group, Research Centre for Natural Sciences, Budapest, Hungary

Correspondence
Tamás Beke-Somfai and Imola Cs. Szigyártó, Institute of Materials and Environmental Chemistry, Biomolecular Self-assembly Research Group, Research Centre for Natural Sciences, Budapest, Hungary.
Email: beke-somfai.tamas@ttk.hu

Email: szigyarto.imola.csilla@ttk.hu

Funding information
Eötvös Loránd Research Network, Hungary, Grant/Award Number: KEP-5/2021,SA-87/2021; National Research, Development and Innovation Office, Ministry of Innovation and Technology of Hungary, Grant/Award Number: 2019-2.1.11-TÉT-2019-00091,2020-1-1-2-PIACI-KFI_2020-00021,TKP2021-EGA-31,KKP_22144180; Hungarian Academy of Sciences, Grant/Award Number: János Bolyai Research Scholarship for Z.V.

Abstract

In the last years, extracellular vesicles (EVs), secreted by various cells and body fluids have shown extreme potential in biomedical applications. Increasing number of studies suggest that a protein corona could adhere to the surface of EVs which can have a fundamental effect on their function, targeting and therapeutical efficacy. However, removing and identifying these corona members is currently a challenging task to achieve. In this study we have employed red blood cell-derived extracellular vesicles (REVs) as a model system and three membrane active antimicrobial peptides (AMPs), LL-37, FK-16 and CM15, to test whether they can be used to remove protein corona members from the surface of vesicles. These AMPs were reported to preferentially exert their membrane-related activity via one of the common helical surface-covering models and do not significantly affect the interior of lipid bilayer bodies. The interaction between the peptides and the REVs was followed by biophysical techniques, such as flow-linear dichroism spectroscopy which provided the effective applicable peptide concentration for protein removal. REV samples were then subjected to subsequent size exclusion chromatography and to proteomics analysis. Based on the comparison of control REVs with the peptide treated samples, seventeen proteins were identified as external protein corona members. From the three investigated AMPs, FK-16 can be considered as the best candidate to further optimize EV-related applicability of AMPs. Our results on the REV model system envisage that membrane active peptides may become a useful set of tools in engineering and modifying surfaces of EVs and other lipid-based natural particles.

KEYWORDS
extracellular vesicles, membrane active antimicrobial peptide, protein analysis, protein corona, spectroscopy

1 | INTRODUCTION

Extracellular vesicles (EVs) are lipid bilayer enclosed nanoparticles released from the multivesicular bodies via exocytosis, or from the cell membrane by membrane budding. These species can also be found in body fluids including serum, plasma, urine, saliva, and breast milk (Cheng & Hill, 2022; Valadi et al., 2007; Xu et al., 2021). They play important roles in intracellular communication, by trafficking cellular contents including proteins, RNA and DNA within their vesicular body, but they also have the advantage of displaying membrane proteins on their external surface (Ko & Naora, 2020; Yang et al., 2018). Due to this widespread molecular cargo, there is an extreme diagnostic potential in EVs liquid biopsies (Killingsworth et al., 2021; Zhou et al., 2020). However, recently increasingly growing evidence suggests that EVs, akin to synthetic nanoparticles, are exposed to spontaneously adsorbing "contaminations" from the protein-rich blood matrix. These adsorbed proteins can be strongly bound, or they can only adhere loosely to the surface and not only in one layer are present on the particle surfaces (Bai et al. 2021). These layers has been identified as 'protein corona' whose formation are influenced by the nature of the biological environment, and also by the physical and chemical properties of the particles. Based on proteomic analysis, it has been observed that EVs also contain certain proteins such as apolipoproteins and immunoglobulins, protein complexes, enzymes and larger aggregates in such a protein corona (Buzas, 2022; Buzás et al., 2018; Palviainen et al., 2020; Yerneni et al., 2022).Therefore, the composition, modulation and characterization of protein corona are essential and need to be addressed, as can influence the nanoparticle bioavailability, bio-distribution (Németh et al., 2017; Nguyen & Lee, 2017; Sung et al., 2015; Wheeler et al., 2021) as well as will improve their applicability in EV-based therapy (Chakraborty et al., 2020; Wang et al., 2021; Wolf et al., 2022). A recent, important study has also demonstrated that protein corona can be formed on purified vesicles upon inserting them into blood plasma (Tóth et al., 2021). Moreover, Wolf and co-workers has been demonstrated the presence of an imageable functional corona around EVs from placental-expanded stromal cells (Wolf et al., 2022) and they show recently, that loss of corona can be restored by using the late SEC fraction (Gomes et al., 2022). Note, that the particular interest towards EV protein corona formation goes beyond purification considerations, as these species could supplement exploration of the EV interaction networks and could also help in understanding basic biophysical and morphologic properties of these vesicles, such as lipid composition, rigidity or EV maturation (Bebesi et al., 2022; Singh et al., 2020; Szigyártó et al., 2018). However, EV corona analysis and its separation from EVs face several difficulties starting from the heterogeneous origin of host EVs, through the presence of non-vesicular protein patches, to the fact that both external and internal proteins on EVs are mostly from the same host organism. Thus, a routine process that separates protein corona from EVs and identifies their composition would be greatly beneficial. Nevertheless, so far efficient biomolecular methods for engineering EV surfaces are lacking. In this respect, we have recently demonstrated that some membrane-active peptides may approach the surface of a lipid bilayer in such a manner that can remove associated proteins from EV surfaces (Singh et al., 2020). This process can be easily followed by polarized light spectroscopy methods (Szigyártó et al., 2018) and some peptides are much more active in removal of these proteins than others (Quemé-Peña et al., 2021). In this respect, we hypothesized that the significant efforts made in the last decades to better understand mechanistic aspects of membrane active antimicrobial peptides (AMPs) could be of great advantage. The interaction of AMPs with the cell membrane can occur through different models, such as through accumulation of peptides on the surface (carpet model), or by membrane association and then inserting into the lipid bilayers (barrel stave and toroidal pore models) (Hancock & Rozek, 2002; Huan et al., 2020). Accordingly, we have selected well-characterized AMPs, which are known to exert their membrane activity by having a phase of surface-coverage, with a helical conformation parallel to the membrane surface (Table 1 and Scheme 1). We have addressed their capacity to remove the surface-associated proteins from red blood cell-derived extracellular vesicles (REVs). For this purpose, REVs were isolated using differential centrifugation steps followed by size exclusion chromatography (SEC) and characterized using transmission electron microscopy, dynamic light scattering and microfluidic resistive pulse sensing (MRPS). Total protein analysis and quantification were performed using circular dichroism and infrared spectroscopy, proteomic analysis as well as Bradford colorimetric assay. Linear dichroism (LD) spectroscopy was used to determine the effective applicable peptide concentration for surface protein removal. Freshly, purified REV samples were submitted to proteomic analysis allowing the identification of seventeen proteins, which we assigned as protein corona members. These results could open novel applications in nanoparticle surface engineering and in EV-based therapeutics research.

TABLE 1 Sequences and properties of the selected membrane-active peptides

Peptide name	Sequence	Net charge	Length	Origin
CM15	KWKLFKKIGAVLKVL	+6	15	Synthetic hybrid, cecropin-melittin derived
LL-37	LLGDFFRKSKEKIGKEFKRIVQRIKDFLRNLVPRTES	+6	37	*Human*, skin and intestine
FK-16	FKRIVQRIKDFLRNLV	+5	16	*Active fragment of LL-37, synthetic*

Net charge refers to pH 7. Note that peptides are amidated at C-terminus.

2 | MATERIALS AND METHODS

A schematic illustration of the experimental work is depicted in Figure S1. The proteomics data has been submitted to the MassIVE data repository with the ID: MSV000089531. We have also submitted all relevant experimental data to the EV-TRACK knowledgebase (EV-TRACK ID: EV220311) (Van Deun et al., 2017). Venn diagrams were made by FunRich Functional Enrichment Analysis Tool (version 3.1.4, (Fonseka et al., 2021; Pathan et al., 2017; 2015)). Graphical abstract was created with BioRender.com.

2.1 | Materials

LL-37 and FK-16 were purchased from NovoPro BioScience Inc. (Shanghai, China). CM15 was provided by the Research Group of Peptide Chemistry, Eötvös Loránd University. Peptides lyophilized powder were dissolved in high-purity water (MilliQ) at 1 mM concentration, aliquoted and stored at −18°C.

2.1.1 | Red blood cell derived EVs (REVs) isolation

The usage of human blood samples was approved by the Scientific and Research Ethics Committee of the Hungarian Medical Research Council (ETT TUKEB IV/701-3/2022/EKU) and during all investigations we followed the guidelines and regulations of the declaration of Helsinki. Healthy donors with informed consent were involved in our studies.

REVs were isolated from 15 ml blood collected from three independent healthy adult donors in tripotassium ethylenediaminetetraacetic acid (K3EDTA) tubes (Greiner). In the first step red blood cells (RBCs) were isolated by centrifugation at 2500 × *g* for 10 mins at 4°C (Nüve NF 800R centrifuge) and were washed with physiological salt solution at least three times at 2500 × *g* for 10 min, 4°C to completely remove platelets and buffy coat. Buffy coat free RBCs were diluted in equal volume of 0.2 μm filtered phosphate buffered saline (PBS, pH 7.4) and stored for 7 days at 4°C. Based on our previous results (Bebesi et al., 2022), the 1-week storage time in PBS buffer produce the formation of mainly monodisperse vesicles, in contrast to the early storage time, where bimodal size distribution and lower particle concentration was observed. Owing to the formation of different vesicle subpopulation, the REVs are isolated after 7 days' storage, according to our standard protocol. During this storage time, surface proteins will also be adsorbed on the vesicles as indicated by previous studies (Singh et al., 2020; Szigyártó et al., 2018). In the second step, after the end of the incubation period (7 days), the cells and the cellular debris were removed by differential centrifugation steps at 2500 × *g* for 15 min and 3000 × *g* for 30 min at room temperature (RT). The supernatant was aliquoted into 2 mL eppendorf tubes and centrifuged at 16000 × *g* for 30 min at 4°C (Eppendorf 5415R, F45-24-11 rotor), after which the pellet was re-suspended in 100 μL PBS.

For spectroscopic studies, the REV samples were further purified with size-exclusion chromatography (SEC) using a 3.5 mL gravity column filled with Sepharose CL-2B gel (GE Healthcare, Sweden). 100 μL of REV sample was loaded onto the top of column followed by the addition of PBS (900 μL) while the flow-through was discarded. The purified REV was eluted with 1 mL PBS and collected. We have previously demonstrated the stability of stored REVs at 4°C, using linear dichroism spectroscopy method (Szigyártó et al., 2018). We observed that the positive peak of the haemoglobin proteins (∼ 420 nm) detaches from the membrane in a time-dependent manner during storage. Therefore, all measurements were performed from freshly isolated samples, stored at 4°C and used within 48 hours after isolation to avoid changes in the REV structure.

2.2 | Methods

2.2.1 | Linear dichroism spectroscopy (LD)

LD spectroscopy is defined as the difference in absorption of the light polarized parallel and perpendicular to the orientation axis (Equation 1) (Nordén, Rodger & Dafforn, 2010; Rodger et al., 2002).

$$LD = A_{\parallel} - A_{\perp} \tag{1}$$

LD gives information about orientation of chromophores relative to the macroscopic orientation axis of the system. The method is used with systems that are either intrinsically oriented or can be oriented during the measurement. Coupled to a Couette flow cell, where a shear gradient is created the vesicles can be distorted. LD measurements were performed at RT on a JASCO-1500 spectropolarimeter equipped with a Couette flow cell system (CFC-573 Couette cell holder). Spectra were collected

between 200 and 600 nm, at a rate of 100 nm/min with a data pitch of 0.5 nm, response time of 1 s, and 1 nm bandwidth. The samples were oriented under a shear gradient of 2270 s^{-1}. Baselines at zero shear gradients were measured and subtracted from all spectra. All measurements were performed in triplicate.

2.2.2 | Circular dichroism spectroscopy (CD)

CD spectra were collected using a Jasco J-1500 spectropolarimeter at RT, between 200 and 270 nm, in a 0.1 cm path length rectangular quartz cuvette (Hellma, USA) at a scan speed of 100 nm/min, with a data pitch of 0.5 nm, 1 nm bandwidth and 3 times accumulation. Spectra was corrected by subtracting the CD curve of PBS buffer. CD measurements were performed in triplicates.

2.2.3 | Flow cytometry (FCM)

Flow cytometric detection of RBC cells was performed with a CytoFlex flow cytometer (Beckman Coulter Inc, Brea, California, USA) using the CytExpert program. Cell count were measured before and after REV production. Cells were washed three times with physiological salt solution and then the buffy coat free RBCs were diluted twice in phosphate buffered saline. During REV production the RBCs were stored vertically in 15 mL centrifuge tubes at 4°C. Events with smaller side- and forward-scatter (SSC and FSC) outside of the cell gate, but larger than the background cytometer noise were considered as cell debris or microparticles. The samples were diluted 10,000× times with PBS buffer, and a flow rate of 10 μL/min was used. Data analysis was performed by Kaluza Analysis Software (Beckman Coulter).

2.2.4 | Transmission electron microscopy combined with freeze fracture (TEM)

Freeze-fracture combined TEM was used to characterize the EVs morphology. Briefly, REV sample was mixed with glycerol in 3:1 volume ratio (Sigma-Aldrich, Hungary). 2 μL of the sample was pipetted onto a gold sample holder and frozen by placing it immediately into partially solidified Freon for 20 s. Fracturing was performed at −100°C in a Balzers freeze-fracture device (Balzers BAF 400D, Balzers AG, Liechtenstein). The replica of the fractured surfaces was made using platinum-carbon evaporation and then cleaned and washed with a water solution of surfactant and distilled water. The platinum-carbon replica was placed onto a 200 mesh copper grid. Measurement was performed in a MORGAGNI 268D (FEI, The Netherlands) transmission electron microscope.

2.2.5 | Dynamic light scattering (DLS)

Particle size and size distribution of REVs were measured at RT using a W130i dynamic light scattering device (DLS, Avid Nano Ltd., High Wycombe, UK) with a diode laser (660 nm) and a photodiode detector. 80 μL samples were placed in low volume disposable cuvettes with 1 cm path-length (UVette, Eppendorf Austria GmbH). The time-dependent autocorrelation function was measured for 10 s and repeated 10 times. Data analysis were performed using the i-Size 3.0 software.

2.2.6 | Microfluidic resistive pulse sensing (MRPS)

The quantitative size distribution and concentration of REVs was measured with MRPS technique using a Spectradyne nCS1 instrument (Spectradyne LLC, USA) and utilizing single-use polydimethylsiloxane cartridges, TS-400 (measurement range 65–400 nm). REV samples were diluted with bovine serum albumin (BSA, Sigma-Aldrich, Hungary) solution (1 mg/mL in PBS buffer), filtered through a VivaSpin 500 (100 kDa MWCO membrane filter, Sartorius, Germany) according to the manufacturer's guidelines. After AMP additions to REVs, all samples were filtered through on a 0.45 μm filter (Corning Costar Spin-X, Sigma-Aldrich) avoiding clogging of the cartridge pores. Control REV was measured in triplicates, whereas each other sample was measured in duplicates.

2.2.7 | Determination of protein concentration and protein to lipid ratio

Protein concentration was determined using Bradford assay according to manufacturer's protocol (Bio-Rad, Hungary). Briefly, in a 96 well plate, 10 μL of REV and standard sample solution were added to 250 μL of Coomassie Brilliant Blue G-250 dye and incubated at RT for at least 5 min. After the incubation time the absorbance was read at 595 nm with a BioTek Synergy 2 plate

reader. Bovine serum albumin (BSA, 2 mg/mL, Bio-Rad) was used as standard, from which eight consecutive dilution steps were made. Each measurements were performed in triplicates.

A spectroscopic protein-to-lipid ratio of REV sample was calculated based on the ratio of the integrated area of amide I band (~1654 cm^{-1}, characteristic for protein content) and of C-H stretching region (3040–2800 cm^{-1}, characteristic for phospholipid content). Attenuated total reflection infrared spectroscopy (ATR-IR, Varian 2000 FTIR Scimitar Series Spectrometer, equipped with a liquid nitrogen cooled mercury-cadmium-telluride detector and with a "Golden Gate" single reflection diamond ATR accessory) measurements were performed to collect the spectra. Briefly, 3 μL of REV sample was mounted onto the ATR surface and immediately after drying (RT, approx. 5 min) the spectra of the thin dry film were collected (64 scans and at a nominal resolution of 2 cm^{-1}). After data acquisition ATR correction, buffer background subtraction and baseline corrections were performed using GRAMS/32 software package (Galactic Inc., USA). For peak identification and area calculation Origin software package (OriginLab, Northampton, MA, USA) was used.

2.2.8 | Sample preparation for mass spectrometry (MS) measurements

REV samples after AMP addition were separated from other constituents, including soluble proteins and destroyed vesicle fragments using Sepharose CL-2B cross-linked agarose gel as stationary phase (GE Healthcare Bio-Sciences AB, Sweden). 50 μL of REV samples were injected into a Jasco HPLC system (Jasco, Tokyo, Japan) consisting of a PU-2089 pump with a UV-2075 UV/Vis and FP-2020 fluorescence detectors controlled by the Chromnav software. The Tricorn 5/100 glass columns (GE Healthcare Bio-Sciences Sweden) filled with Sepharose CL-2B were used with a flow rate of 0.5 mL/min and PBS as eluent. Absorbance chromatograms were recorded at 280 nm and REVs eluted in the first peak were collected. The area under the curve (AUC) of the REV peak was used to quantify the amount of vesicles.

PD MiniTrap desalting columns (Sigma Aldrich) were used according to the instructions of the manufacturer. After column equilibration with high-purity water (MilliQ), 500 μL of REV sample was added to the column and eluted with 1 mL of MilliQ. Samples were snap freezed and subjected to MS analysis.

2.2.9 | Proteomics

REVs were prepared as described above and stored frozen at −80°C in MilliQ water. Repeated freeze-thaw cycles (Turiák, Misják et al., 2011) were used to extract proteins from the vesicle samples. 10 μg aliquots were digested using a tryptic digestion protocol (Turiák, Ozohanics et al., 2011). NanoLC-MS/MS analysis was carried out on 1 μg digests using a Dionex Ultimate 3000 nanoRSLC (Dionex, Sunnyvale, Ca, USA) coupled to a Bruker Maxis II mass spectrometer (Bruker Daltonics GmbH, Bremen, Germany) via Captive Spray nanobooster ionsource. Peptides were trapped on an Acclaim PepMap100 C18 (5 μm, 100 μm × 20 mm, Thermo Fisher Scientific, Waltham, MA) column and then separated on an Acquity M-Class BEH130 C18 analytical column (1.7 μm, 75 μm × 250 mm Waters, Milford, MA) using gradient elution. For data dependent acquisition a fix cycle time of 2.5 s was used. Raw data files were processed using the Compass Data Analysis software (Bruker, Bremen, Germany). MaxQuant software (Cox and Mann 2008) (version 1.6.17.0) was used for label-free quantitation using its Andromeda search engine. For the Andromeda search, a focused database was used, which was created following protein search on Byonic software (v3.6.0, Protein Metrics Inc, San Carlos, CA, USA) against the Swissprot Homo sapiens database applying the following search parameters: precursor mass tolerance 20 ppm, fragment mass tolerance 40 ppm, cleavage at lysine and arginine C terminal, maximum two missed cleavages, and 2% FDR limit. Keratins were considered as potential contaminants and omitted from the list. To exclude that presence of some proteins is detected due to mere sequential overlapping with the employed membrane active peptides, we have performed a systematic analysis of short sequential regions from the selected AMPs on the identified proteins. This analysis resulted no match for the found protein sequences, excluding artifacts due to overlaps with any of the AMP sequences. The identified proteins of control REV (REV_summ) are the average of three parallel measurements.

3 | RESULTS

3.1 | Selection strategy for employed AMPs

The family of antimicrobial peptides (AMPs) typically have a short sequence (10–50 residues), most often a net positive charge usually between +2 to +9, and contain ~ 50% hydrophobic residues making them membrane-active (Mangoni et al., 2015; Nayab et al., 2022). The innate immune system secretes gene-encoded AMPs which are effective against bacteria, fungi, viruses and some of them have shown anticancer activities as well (Huan et al., 2020; Pirtskhalava et al., 2021). For EV interactions, the above properties deemed particularly useful, as AMPs form a favourable electrostatic interaction with negatively charged lipid

bilayer surfaces (van der Koog et al., 2022). The lipid composition of EVs show some differences based on their origin, however an enrichment of sphingolipids, cholesterol and anionic phospholipids, particularly phosphatidylserine were reported (Skotland et al., 2020). They also show similarities with bacterial and cancer cell membranes, due to the presence of negatively charged lipids and to glycan-moieties (Tissot et al., 2013; Williams et al., 2019). Within the several action mechanisms of AMPs (Brogden, 2005), we primarily focused on peptides that have recently been identified to exert their activity similarly to the "carpet model" mechanism (Hancock & Rozek, 2002; Huan et al., 2020; Quemé-Peña et al., 2021). For our current investigation, we selected three well-characterized antimicrobial peptides: LL-37, FK-16 and CM15. The latter was included based on previously reported results (Singh et al., 2020) which showed that the natural AMP, melittin, derived from bee venom, and its synthetic derivative, CM15, had the capacity of removing proteins from REV membrane surfaces. These results provided also the means to follow how AMPs can remove proteins from the surface of EVs, such as haemoglobin, a major EV surface component, which has an absorption peak that can be tracked by polarized light spectroscopy techniques (Szigyártó et al., 2018). Haemoglobin subunits are the main components of adsorbed proteins formed in vivo on the surface of engineered nanoparticles immediately after entering into body (Hadjidemetriou et al., 2016; Hadjidemetriou et al., 2015; Hadjidemetriou & Kostarelos, 2017; Sakulkhu et al., 2014; Zhang et al., 2018). For more detailed considerations, CM15 is a synthetic hybrid peptide derived from the natural AMP cecropin and melittin, and it is known to act primarily by associating with the membrane in a helical form oriented parallel to the membrane surface, akin to a carpet model (Pistolesi et al., 2007; Wang et al., 2012), though pore formation was also reported for this peptide (Milani et al., 2009). The human cathelicidin peptide LL-37 exhibits broad spectrum activities against bacteria, fungi and viruses (Tripathi et al., 2015; Vandamme et al., 2012; Zsila et al., 2019). Besides antimicrobial activities, it also plays important roles in biofilm inhibition, in regulating the immune response, tissue repair and wound healing (Kang, Dietz & Li, 2019; Verjans et al., 2016; Wang et al., 2019; Wang 2008). Due to its cationic and hydrophobic character the peptide causes perturbations in lipid order and packing, covering the external layer of membrane and at a high concentration leading to membrane disintegration (Henzler-Wildman et al., 2004; Majewska et al., 2021). We have recently identified, that for synthetic liposomes with phosphatidyl-serine content and an average size of 100 nm, these mostly tether the surface similar to the carpet model (Quemé-Peña et al., 2021). Finally, the active fragment of LL-37 (FK-16) was also involved in this study. FK-16 was reported to inhibit the growth of various bacteria strains and cancer cells (Li et al., 2006). Moreover, it has been also demonstrated a significant anti-biofilm activity against *S. aureus* and *E. coli* (Mishra & Wang, 2017). Recently, we have also investigated its effect on model systems, which resulted in a preferential surface-coverage for this peptide as well, similar to a carpet model mechanism.

3.2 | Assessment of effective peptide concentration for surface treatment of EVs

The effectiveness of isolation and the presence of EVs in the sample was confirmed by morphological characterization using freeze-facture combined transmission electron microscopy (TEM) and dynamic light scattering (DLS) techniques. The representative TEM images of REVs with spherical morphology and with granules on their surface representing membrane-associated proteins were detected with an average diameter of ~ 200 nm (Figure S2). We employed microfluidic resistive pulse sensing (MRPS) analysis to determine the concentration and size distribution of vesicles. The overall particle concentration of the REVs was $2.3*10^{12} \pm 2.7*10^{10}$ particles/mL. The total protein concentration was determined by Bradford colorimetric assay resulting in similar value with previous observations (Bebesi et al., 2022; Kitka et al., 2019). Further on, IR spectroscopy was used to calculate the spectroscopic protein-to-lipid ratio as a parameter for EV characterization. The representative IR spectra of REV sample (Figure S3) shows the characteristic bands of proteins (amide I and amide II, from 1700 to 1500 cm^{-1} and amide A ~ 3295 cm^{-1}), of phospholipids (lipid acyl chains, from 3040 to 2800 cm^{-1} and ester carbonyl group of phospholipids ~1737 cm^{-1}) and of the fingerprint region attributed to phosphodiester groups and phosphate vibrations of the PBS buffer (from 1300 to 1000 cm^{-1}). The protein-to-lipid ratio was determined as the ratio of integrated areas of amide I band and of the C-H stretching bands, which value (1.7 ± 0.2) is in good agreement with our previous results (Bebesi et al., 2022).

Another optical technique, CD spectroscopy, was used to characterize the structural properties of REV proteins. We have previously reported the changes in protein secondary structure after AMPs treatment (Quemé-Peña et al., 2021; Singh et al., 2020; Szigyártó et al., 2018). The typical REV CD spectra exhibits a broad negative band at 226 nm originated from n-π^* transition with a weaker unresolved π-π^* shoulder at ~210 nm (Figure S4), which is in good agreement with our earlier results and support the reproducibility of our isolation protocol.

Washed RBCs were also examined before and after REV production (Figure S5), as a control experiment to determine changes in the number of intact cells during storage. A small decrease (~ 5%) was detected in the intact RBC number during the storage for seven days at 4°C.

Based on proteomic results we have identified EV markers from categories 1 and 2 as well as non-EV markers (category 3) based on the MISEV2018 guidelines (Théry et al., 2018), such as CD55, CD47 and CD59, GYPA, ACHE, FLOT1 and FLOT2. Non-EV markers such as keratins and albumin were present in our MS data, however keratins were omitted from the protein list as potential contamination. A more detailed analysis of the identified proteins and protein corona members, which is the main focus of our work, is included in the discussion section.

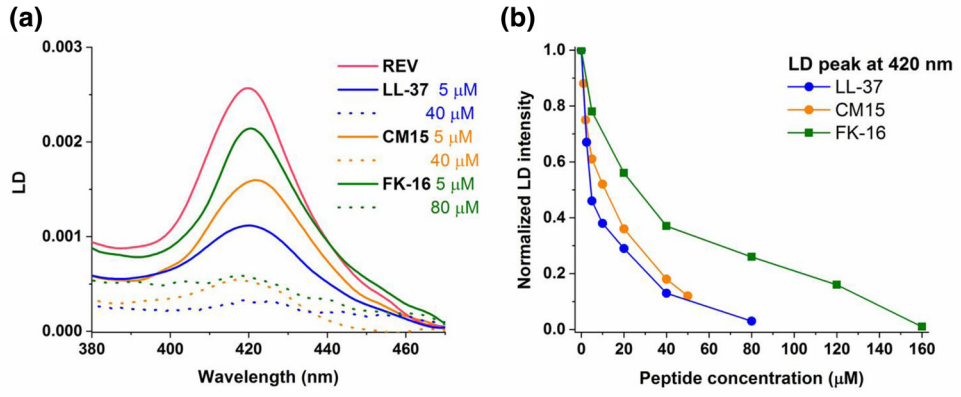

FIGURE 1 REV—AMP interactions studied by LD spectroscopy. (a) Signal intensity changes at the Soret band of REV samples upon addition of LL-37 (blue), CM15 (orange) and FK-16 (olive). For better visualization selected peptide concentrations are showed. (b) LD peak intensity at 420 nm as a function of AMPs. Data are normalized to the LD intensity of control REV.

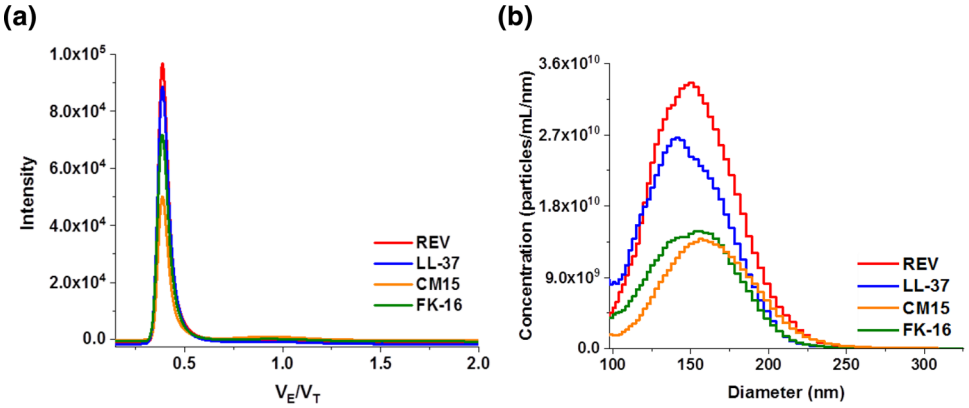

FIGURE 2 Characterization of REV samples after AMP treatment. (a) Size exclusion HPLC chromatogram of vesicle samples at 280 nm. REVs were eluted at 0.38 V_E/V_T (V_E = elution volume, V_T = total volume). Chromatograms were collected after addition of 80 μM for LL-37 and CM15 and 160 μM for FK-16, respectively. (b) Concentration and size distribution of REV samples measured by microfluidic resistive pulse sensing (MRPS). Peptide concentrations were 80 μM for LL-37 and CM15 and 160 μM for FK-16, respectively. Both techniques indicate that significant amount of REVs are retained after treatment with AMPs.

As reported earlier, the structural effect of the selected peptides on REVs were followed by flow-LD spectroscopy (Quemé-Peña et al., 2021; Singh et al., 2020). The LD spectrum of control REVs shows two major peaks, one at ~220 nm, arising mostly from a mixture of the n-π^* and π-π^* amide transitions of proteins, and another at ~420 nm, corresponding to the Soret band of haemoglobins (Szigyártó et al., 2018). Titration of REVs with increasing AMP concentrations was used to determine the effective peptide concentration which resulted in detachment of surface proteins (Figure S6).

All measurements were performed immediately after AMP additions to avoid the time dependent aggregation and pore formation on REVs. A gradual decrease at 420 nm, the contribution from surface-attached haemoglobin (Figure 1), and at 220 nm (Figure S6D) were observed for all selected peptides. The most significant effect was detected for the peptide LL-37, where the 5 μM concentration resulted in the reduction of the peak intensity by ~ 50%, while further addition of peptide up to 80 μM led to complete loss of the signal intensity. A very similar trend was detected also for the CM15. In contrast, a higher concentration was required for FK-16 to up 160 μM to reach the same loss of intensity.

Based on these results and the analysed loss of band intensity at 420 nm, for LL-37 and CM15 we decided to apply 80 μM, while for FK-16 160 μM peptide concentration, as for these values we observed a near complete loss of protein signals in LD spectral intensity (Figure 1b and Figure S6D), indicating that majority of the marker surface proteins were removed.

3.3 | Effect of the peptide concentration on the size and concentration of EVs

Size exclusion chromatography measurements were performed to separate the intact vesicle from protein-rich soluble fractions and compare the effect of peptides on REVs using the selected concentrations. Figure 2a shows the absorbance chromatogram

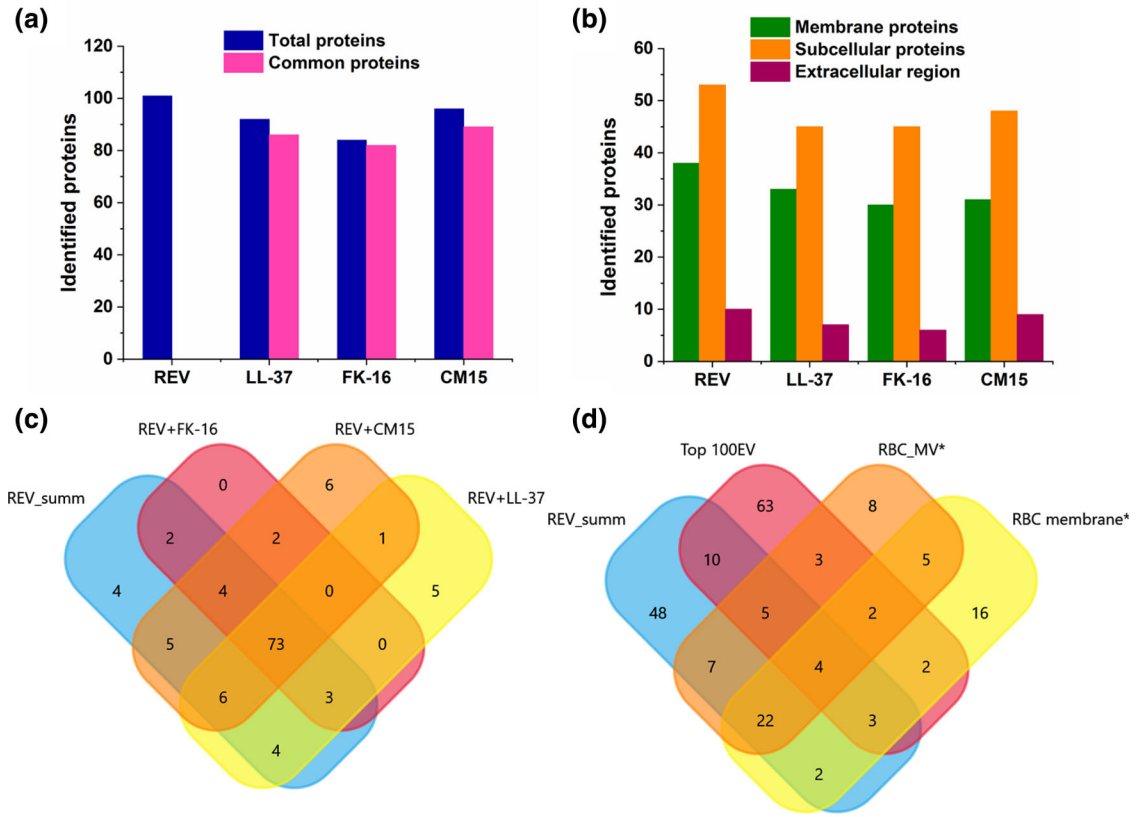

FIGURE 3 Protein composition of the REV samples after AMP treatment. (a) Total and common proteins identified (common proteins are present in both control and AMP treated REV samples). (b) Classification of the identified proteins for each sample. (c) Venn diagram of overlapping proteins from control and AMP treated REV samples. (d) Comparison of proteins from Vesiclepedia Top 100EV with proteins of red blood cells membranes (RBC membrane*) and RBC-MV* (*data from Prudent et al., 2018) as well as with REV proteins (REV_summ). The bar graphs demonstrate that vast majority of initial proteins are retained for AMP treated samples, which confirms that the vesicles remained largely intact. For all protein categories a slight decrease can be seen for the AMP-treated samples suggesting that the peptides affect only a small subsection of the total protein content.

recorded at 280 nm of the control REVs and in the presence of peptides, where the peak at 0.38 V_E/V_T (V_E = elution volume, V_T = total volume) correspond to the intact vesicles. Based on our previous work (Kitka et al., 2019), the area under the curve (AUC) values could be associated with the vesicle concentration. In comparison with control REV, a decrease in vesicle concentration can be detected after the addition of AMPs, though the resulting vesicle amount is still suitable for proteomic analysis. In connection with this, we noticed in the absorbance chromatogram of the selected AMPs, a very small second peak (Figure 2a, peak ~ 0.93 V_E/V_T), which could correspond to free proteins and vesicle fragments, however, it proved to have a negligible protein content and was unsuitable for proteomic analysis.

Microfluidic resistive pulse sensing (MRPS) was used to determine the effect of AMPs on size distribution and concentration of REVs. The overall concentration of the control sample was $(2.3 \pm 0.027) \times 10^{12}$ particles/mL (Figure 2b, Table S1) with a mean diameter of 162.6 ± 0.7 nm which is in line with our previous results (Bebesi et al., 2022). A slight decrease in vesicle concentration were detected in the presence of AMPs using the above defined peptide concentrations, while particle size distribution remained mostly similar after addition of peptides. These results suggest that the treatment of REV with selected AMPs resulted in slight changes, however most of the vesicles remained intact.

3.4 | AMP specificity in proteins removal

Nanoscale liquid chromatography coupled to tandem mass spectrometry (nano LC-MS/MS) is an essential tool for proteomic analysis. Here the REVs were mixed with the selected antimicrobial peptides at the identified concentrations and after 5 min incubation period the samples were purified using HPLC-SEC and the intact vesicles were collected. Prior to MS analysis the PBS buffer was exchanged to water using a desalting column. Based on proteomic results a total number of 101 proteins were identified in the control REV sample (Figure 3a,c and Table SI_identified proteins), including numerous membrane-bound proteins, cytosolic proteins, metabolic enzymes and haemoglobins (Figure 3b and Table S2) from which 27 are considered the most

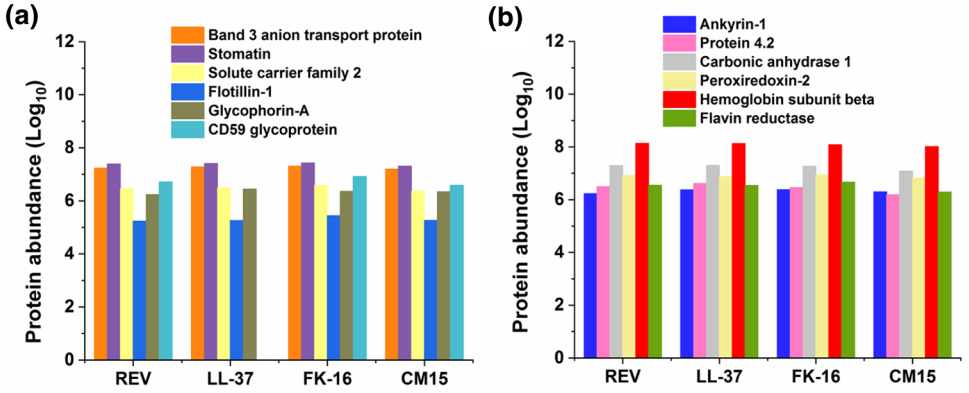

FIGURE 4 Proteomic differences of selected most abundant proteins in control and in AMP-treated samples. (a) Characteristic proteins of the RBC membrane and of (b) subcellular origin were selected. The bar graphs demonstrate that almost all initial proteins are present after AMP treatment, in similar abundance as in control samples.

abundant proteins of red blood cell membranes (Bosman et al., 2008; Pham et al., 2021; Prudent et al., 2018; Thangaraju et al., 2021). The proteins found here were searched in the Vesiclepedia and ExoCarta (Kalra et al., 2012; Keerthikumar et al., 2016) databases to confirm their presence in the EV entries, while their predicted membrane or cellular localization was identified using the UniProt database (The UniProt Consortium, 2021). In order to compare our proteomics results with the list of proteins from related publications the UniProt protein IDs were converted to gene symbols (Tables S3 and S4). The identified proteins of control REV (REV_summ) were compared with proteins of AMP-treated samples, which revealed ~90 "common proteins" (Figure 3a,c) supporting that addition of AMPs had no drastic effect on the protein abundance for the identified REV proteins. We have compared our data with previously published results on the number of proteins from the RBC-derived vesicles and RBC membrane (Bosman et al., 2008; Prudent et al., 2018). The Venn diagram shows the overlap of proteins in good correlation with those identified in stored RBC and microvesicles (Figure 3d). Forty-three proteins were common to both total membrane proteins and vesicles. With few exceptions, the identified control REV proteins were present in the red blood cells hits of Vesiclepedia database (Kalra et al., 2012). We then searched the REV_summ proteins with the entries of TOP 100EV proteins in Vesiclepedia, which resulted in an overlap of 22 proteins (Figure 3d). It should be noted that the list of TOP100 refers to the most often detected proteins in all EV studies without defining whether they are marker EV proteins or experimental by-products (Pathan et al., 2019).

To eliminate potential mechanistic variations of the individual peptides used, we assumed that those proteins which are removed from REVs by at least two of the AMPs used here, could be considered as members of the protein corona. To avoid misinterpretations, special focus was also given on understanding whether changes can be observed upon AMP treatment for those key proteins that have known position and function in red blood cells. Accordingly, first the relative abundance of the membrane proteins were investigated.

It can be seen, that for six selected characteristic RBC membrane proteins their abundance remained constant after LL-37, FK-16 and CM15 treatment, with only exception of CD59 glycoprotein, which was removed by LL-37 (Figure 4a). Furthermore, we have identified 31 membrane proteins, which were not affected by AMP treatment, indicating that the selected peptides do not interfere significantly with membrane inserted proteins (Figure 3b). Besides the presence of membrane proteins, the proteomic data also confirmed the presence of a high number of subcellular proteins in all investigated samples (Figures 3b and 4b), with only minor differences in the relative abundance of these. This overall resulted in 47 identified subcellular proteins, which were not affected significantly by the AMP treatment. The presence of these membrane and subcellular proteins validate the strong selectivity of the used AMPs toward surface proteins as neither significant membrane disruption (resulting in drastic loss of membrane proteins), nor large pore formation (resulting in loss of internal subcellular proteins) influenced the overall proteomic results. Once, these results showed that AMPs do not affect the above two main groups of proteins in REVs, the list of proteins detected for treated samples were subtracted from the list of control REV samples leading in 17 proteins identified as part of the EV corona (Figure 5, Table 2).

4 | DISCUSSION

Although the current focus of this study was to demonstrate that AMPs are suitable to remove and separate protein corona members from EVs, some considerations should be made on the employed EV model system and also on the proteins that were considered as corona members. During the RBC lifespan, vesiculation is the process taking place both *in vivo* and *in vitro*,

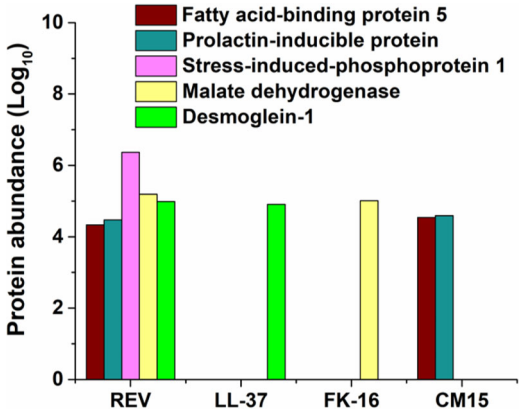

FIGURE 5 Comparison of selected protein corona members 2018; 2021) in control and in AMP-treated samples.

TABLE 2 Identified protein corona members and their cellular localization

PROTEINS	AMP[a]	Protein category
2,3-cyclic-nucleotide 3-phosphodiesterase (CNP)	FK-16, CM15	plasma membrane
Desmoglein-1 (DSG1)	FK-16, CM15	plasma membrane
Low-density lipoprotein receptor-related protein 6 (LRP6)	FK-16, LL-37	plasma membrane
Lymphocyte function-associated antigen 3 (CD58)	LL-37,CM15	plasma membrane
Ecto-ADP-ribosyltransferase 4 (ART4)	FK-16, CM15	plasma membrane
Blood group Rh(D) polypeptide (RHD)	FK-16, CM15	plasma membrane
Cytochrome b reductase 1 (CYBRD1)	FK-16, LL-37	plasma membrane
Fatty acid-binding protein 5 (FABP5)	FK-16, LL-37	extracellular region or secreted
Prolactin-inducible protein (PIP)	FK-16, LL-37	extracellular region or secreted
Human serum albumin (ALB)	LL-37, FK-16, CM15	secreted
Calmodulin-like protein 5 (CALML5)	LL-37, FK-16, CM15	extracellular region
Stress-induced-phosphoprotein 1 (STIP1)	LL-37, FK-16, CM15	subcellular
Malate dehydrogenase (MDH1)	LL-37,CM15	subcellular
Carbonic anhydrase 3 (CA3)	FK-16, LL-37	subcellular
Transketolase (TKT)	LL-37, FK-16, CM15	subcellular
L-lactate dehydrogenase A chain (LDHA)	LL-37, FK-16, CM15	subcellular
Programmed cell death protein 4 (PDCD4)	FK-16, LL-37	subcellular

[a]The AMPs which removed the listed protein based on the proteomics results.

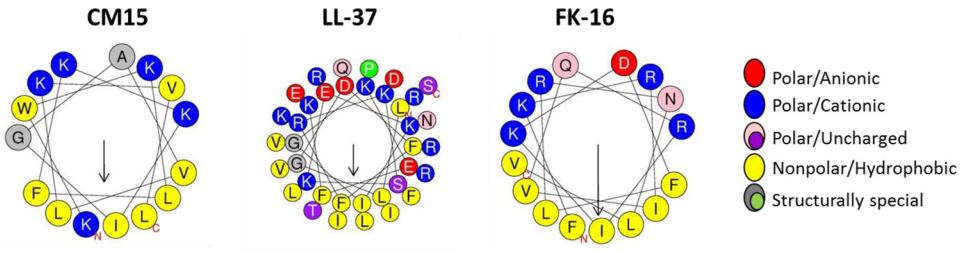

SCHEME 1 Helical wheel diagrams of the peptides used in this study. Diagrams were drawn using HELIQUEST software (Gautier et al., 2008). The arrows indicate the direction of the hydrophobic face.

where damaging components of the erythrocyte membrane are eliminated. Moreover, RBCs suffer irreversible changes during haemolysis, which contribute to the release of internal constituents. Albeit, during the isolation of RBC-derived vesicles we have performed purification steps, which allow the separation of free proteins and membrane fragments from the intact vesicles, nevertheless this will not exclude entirely the presence of free intracellular proteins from the solution. Moreover, using REV as a model system, these proteins could also originate from RBCs during maturation or lysis processes. However, we have confirmed that during REV production only ~ 5% of RBCs are potentially destroyed (Figure S5). While, the above suggest that protein corona could be effected by the employed protocols, nonetheless, it could be valuable and relevant to enlist and compare the detected corona members with studies addressing these components with alternative approaches. The identified protein corona members presented here include seventeen proteins with initial origin from plasma membrane, from cytosol and from extracellular regions (Table 2, Figure S7). Majority of them are components of red blood cells (CYBRD1, RHD, CD58, CA3, DSG1, MDH1, ALB, FABP5, PIP, LDHA, TKT, STIP1), while three of them (PDCD4, LRP6, CALML5) have so far been found in other EVs, mainly originating from different cancer cells (Galuppini et al., 2019; Matsuhashi et al., 2019; Tung et al., 2012; Yuan et al., 2017). We have also found two additional corona members, ART4 and CNP, which could not be found in vesicle databases (Kalra et al., 2012).

When comparing the current findings with the most commonly found protein corona members for EVs and synthetic nanoparticles we found several overlaps, including intracellular proteins, haemoglobins, complement proteins, apolipoproteins and albumin (Chakraborty, Ethiraj & Mukherjee, 2020; Kari et al., 2020; Tóth et al., 2021; Wang et al., 2021). Out of these TKT, PIP, MDH1 and CALML5 are among the most common ones, which was also found here. As mentioned above, we have initially considered as corona members only those proteins, which were removed by at least two of the tested AMPs. When we expand the list to the proteins removed by only one AMP, we have additional proteins (AZGP1, AGO2 and CD55) that were also found as corona members for various nanoparticles. Moreover, there were at least six additional, previously (Kari et al., 2020; Tóth et al., 2021) identified corona members, which had a rather high abundance on REVs, but after AMP treatment their abundance were reduced. The numerous overlaps found above suggest that the current REV isolation protocol results model system that contains a significant amount of protein corona members. It should be noted, that most likely some of the found protein corona members are not in their functional form, as they are likely a result of degradation processes (Bosman et al., 2008; Prudent et al., 2018). The initial results here are hoped to stimulate more application-specific use of membrane-active peptides on EVs. Previous mechanistic findings on CM15, LL-37 and FK-16 were employed here and these models were validated with the current results. The HPLC and MRPS results confirmed that a significant amount of REVs were retained in their original vesicular form and in the average size range of REVs (Figure 2). The proteomics results have shown that most of the proteins that are not on the surface were not affected by these peptides (Figure 4).

Interestingly it should be mentioned that the employed peptides also caused the appearance of several proteins in the proteomics measurements which were not identified for the control REVs (Figure S8). These likely arise from favourable interactions of partially negatively charged areas of the proteins with the cationic lipids, that results in the attachment of these proteins to the REV surfaces with the AMPs acting as membrane anchors. Clearly, additional studies will be needed to better understand the various aspects of the AMP-EV interactions and to identify the most suitable peptides for vesicle surface manipulation. The main characteristics of such a peptide are that it should not have a significant membrane disrupting effect on small vesicles, it should efficiently remove surface proteins, but it would not cause further proteins to attach to the membranes. After addition of FK-16, 15 out of the 17 protein corona members were removed from REV surfaces (Table 2, Figure S7). In contrast, for CM15 only 11 proteins were missing, whereas for LL-37 13 proteins were removed. On the other hand, when considering appearance of additional proteins, we detected six for LL-37, for CM15 seven additional proteins have appeared, whereas for FK-16 only two new proteins have attached to the REV surfaces (Figure S8). Interestingly, when analysing the removed proteins by the three peptides, it can be seen that LL-37 removes only two out of seven identified membrane proteins from the 17 corona members, whereas it removes all water soluble protein corona members with subcellular origin (Figure S7). In contrast, CM15 seemingly shows an opposite tendency, namely it removes more membrane proteins while leaves majority of the water soluble ones intact on the protein corona. In this regard FK-16 seems the most suitable to remove protein corona members as it is equally efficient in removing both membrane and water soluble proteins adsorbed on the EV surface.

Based on the current results, FK-16 seems the most promising peptide which could serve as basis for further development. In addition, the removal of the surface proteins based on the decrease of the corresponding LD peaks (Figure 1 and Figure S6) suggest that a wider range of concentration could be tested for FK-16, allowing for further optimization to find a concentration where membrane disruption is minimal, yet most of the surface proteins are already removed. Moreover, investigation with EVs isolated from additional cell types will also be needed to further assess the surface protein removal efficiency of AMPs.

The interactions described here between AMPs and EVs have another interesting aspect. While nanoparticle engineering by AMPs has clear potential, current results also draw attention to the *in vivo* relevance of EV—host defence peptide interactions. Both EVs and proteins can be found in elevated levels at sites of infection, where mammalian EVs act as transporting agents delivering vital biomolecules for wound healing (Narauskaitė et al., 2021), whereas outer membrane vesicles (OMVs) in the hostile bacterial colonies are responsible for cell-cell communication and delivering components required to mitigate host immune answers (Sartorio et al., 2021). In this respect numerous host peptides are overexpressed at these infectious sites, including LL-37 (Nasseri & Sharifi, 2022). The natural peptide interaction with mammalian EVs at these locations could aid cargo redistribution,

whereas more membrane disrupting AMPs could disrupt EVs and release cytosolic components that are relevant for wound healing. On the other hand it is likely, that tethering bacterial EVs, which carry important components, such as compounds of quorum sensing, could be also relevant for exerting AMP antibiofilm activity (Hancock et al., 2021; Zsila et al., 2021).

5 | CONCLUSION

Our results demonstrate that the selected AMPs, LL-37, FK-16 and CM15 have an affinity for surface covering on membranes and can be used in removing and identification of protein corona components of EVs. The detachment of these proteins opens toward novel applications in nanoparticle surface engineering and in research of EV-based therapeutics. Based on several parameters, FK-16 was found the most efficient for further studies. In the future we aim to expand our investigations to find more suitable peptide candidates. Routine identification of protein corona members could improve our fundamental understanding on EV biology and on their molecular function. It is hoped that the current results will aid use of peptides as engineering tools not only for EVs but also for other biological nanoparticles.

AUTHOR CONTRIBUTION

P.S., I.Cs.Sz. and T.B-S. designed the study. A.G., D.K. and Z.V. performed HPLC and MRPS measurements. P.S., M.Q.P. and M.R. performed and analysed spectroscopy measurements. L.T. and L.D. performed proteomic analysis. All authors were involved in the evaluation of results. I.Cs.Sz., Z.V. and T.B-S. analysed overall results. P.S., I.Cs.Sz. and T.B-S. wrote the paper.

ACKNOWLEDGEMENTS

This work was funded by the Ministry of Innovation and Technology of Hungary through the National Research, Development and Innovation Office, financed under the TKP2021-EGA-31, the 2020-1-1-2-PIACI-KFI_2020-00021, 2019-2.1.11-TÉT-2019-00091 and KKP_22 project no. 144180. Support from Eötvös Loránd Research Network, grant no. SA-87/2021 and KEP-5/2021 is also acknowledged. Z.V. was supported by the János Bolyai Research Scholarship of the Hungarian Academy of Sciences.

CONFLICT OF INTEREST STATEMENT

The authors report no conflict of interest.

ORCID

Priyanka Singh https://orcid.org/0000-0002-8390-7833
Imola Cs. Szigyártó https://orcid.org/0000-0002-8551-8014
Maria Ricci https://orcid.org/0000-0002-8548-5427
Anikó Gaál https://orcid.org/0000-0003-4064-1825
Mayra Maritza Quemé-Peña https://orcid.org/0000-0002-0257-6594
Diána Kitka https://orcid.org/0000-0002-8319-5960
Lívia Fülöp https://orcid.org/0000-0002-8010-0129
Lilla Turiák https://orcid.org/0000-0002-2139-8156
Zoltán Varga https://orcid.org/0000-0002-5741-2669
Tamás Beke-Somfai https://orcid.org/0000-0002-4788-3758

REFERENCES

Bai, X., Wang, J., Mu, Q., & Su, G. (2021). In vivo Protein Corona Formation: Characterizations, Effects on Engineered Nanoparticles' Biobehaviors, and Applications. *Frontiers in Bioengineering and Biotechnology*, 9. https://doi.org/10.3389/fbioe.2021.646708

Bebesi, T., Kitka, D., Gaál, A., Szigyártó, I. C., Deák, R., Beke-Somfai, T., Koprivanacz, K., Juhász, T., Bóta, A., Varga, Z., & Mihály, J. (2022). Storage conditions determine the characteristics of red blood cell derived extracellular vesicles. *Scientific Reports*, *12*(1), 977. https://doi.org/10.1038/s41598-022-04915-7

Bosman, G. J. C. G. M., Lasonder, E., Luten, M., Roerdinkholder-Stoelwinder, B., Novotný, V. M. J., Bos, H., & De Grip, W. J. (2008). The proteome of red cell membranes and vesicles during storage in blood bank conditions: RBC membrane proteome during storage. *Transfusion*, *48*(5), 827–835. https://doi.org/10.1111/j.1537-2995.2007.01630.x-i2

Brogden, K. A. (2005). Antimicrobial peptides: Pore formers or metabolic inhibitors in bacteria? *Nature Reviews Microbiology*, *3*(3), 238–250. https://doi.org/10.1038/nrmicro1098

Buzas, E. I. (2022). Opportunities and challenges in studying the extracellular vesicle corona. *Nature Cell Biology*, *24*(9), 1322–1325. https://doi.org/10.1038/s41556-022-00983-z

Buzás, E. I., Tóth, E. Á., Sódar, B. W., & Szabó-Taylor, K. É. (2018). Molecular interactions at the surface of extracellular vesicles. *Seminars in Immunopathology*, *40*(5), 453–464. https://doi.org/10.1007/s00281-018-0682-0

Chakraborty, D., Ethiraj, K. R., & Mukherjee, A. (2020). Understanding the relevance of protein corona in nanoparticle-based therapeutics and diagnostics. *RSC Advances*, *10*(45), 27161–27172. https://doi.org/10.1039/D0RA05241H

Cheng, L., & Hill, A. F. (2022). Therapeutically harnessing extracellular vesicles. *Nature Reviews Drug Discovery*, *21*(5), 379–399. https://doi.org/10.1038/s41573-022-00410-w

Cox, J., & Mann, M. (2008). MaxQuant enables high peptide identification rates, individualized p.p.b.-range mass accuracies and proteome-wide protein quantification. *Nature Biotechnology*, *26*(12), 1367–1372. https://doi.org/10.1038/nbt.1511

Fonseka, P., Pathan, M., Chitti, S. V., Kang, T., & Mathivanan, S. (2021). FunRich enables enrichment analysis of OMICs datasets. *Journal of Molecular Biology*, *433*(11), 166747. https://doi.org/10.1016/j.jmb.2020.166747

Galuppini, F., Fassan, M., Bertazza, L., Barollo, S., Cascione, L., Watutantrige-Fernando, S., Lazzarin, V., Simonato, P., Vianello, F., Rugge, M., Mian, C., & Pennelli, G. (2019). Programmed cell death 4 (PDCD4) as a novel prognostic marker for papillary thyroid carcinoma. *Cancer Management and Research*, *11*(August), 7845–7855. https://doi.org/10.2147/CMAR.S194344

Gautier, R., Douguet, D., Antonny, B., & Drin, G. (2008). HELIQUEST: A web server to screen sequences with specific -helical properties. *Bioinformatics*, *24*(18), 2101–2102. https://doi.org/10.1093/bioinformatics/btn392

Gomes, F. G., Andrade, A. C., Wolf, M., Hochmann, S., Krisch, L., Maeding, N., Regl, C., Poupardin, R., Ebner-Peking, P., Huber, C. G., Meisner-Kober, N., Schallmoser, K., & Strunk, D. (2022). Synergy of human platelet-derived extracellular vesicles with secretome proteins promotes regenerative functions. *Biomedicines*, *10*(2), 238. https://doi.org/10.3390/biomedicines10020238

Hadjidemetriou, M., Al-Ahmady, Z., & Kostarelos, K. (2016). Time-evolution of in vivo protein corona onto blood-circulating pegylated liposomal doxorubicin (DOXIL) nanoparticles. *Nanoscale*, *8*(13), 6948–6957. https://doi.org/10.1039/C5NR09158F

Hadjidemetriou, M., Al-Ahmady, Z., Mazza, M., Collins, R. F., Dawson, K., & Kostarelos, K. (2015). *In vivo* biomolecule corona around blood-circulating, clinically used and antibody-targeted lipid bilayer nanoscale vesicles. *ACS Nano*, *9*(8), 8142–8156. https://doi.org/10.1021/acsnano.5b03300

Hadjidemetriou, M., & Kostarelos, K. (2017). Evolution of the nanoparticle corona. *Nature Nanotechnology*, *12*(4), 288–290. https://doi.org/10.1038/nnano.2017.61

Hancock, R. E. W., Alford, M. A., & Haney, E. F. (2021). Antibiofilm activity of host defence peptides: Complexity provides opportunities. *Nature Reviews Microbiology*, *19*(12), 786–797. https://doi.org/10.1038/s41579-021-00585-w

Hancock, R. E. W., & Rozek, A. (2002). Role of membranes in the activities of antimicrobial cationic peptides. *FEMS Microbiology Letters*, *206*(2), 143–149. https://doi.org/10.1111/j.1574-6968.2002.tb11000.x

Henzler-Wildman, K. A., Martinez, G. V., Brown, M. F., & Ramamoorthy, A. (2004). Perturbation of the hydrophobic core of lipid bilayers by the human antimicrobial peptide LL-37. *Biochemistry*, *43*(26), 8459–8469. https://doi.org/10.1021/bi036284s

Huan, Y., Kong, Q., Mou, H., & Yi, H. (2020). Antimicrobial peptides: Classification, design, application and research progress in multiple Fields. *Frontiers in Microbiology*, *11*, 582779. https://www.frontiersin.org/article/10.3389/fmicb.2020.582779

Kalra, H., Simpson, R. J., Ji, H., Aikawa, E., Altevogt, P., Askenase, P., Bond, V. C., Borràs, F. E., Breakefield, X., Budnik, V., Buzas, E., Camussi, G., Clayton, A., Cocucci, E., Falcon-Perez, J. M., Gabrielsson, S., Gho, Y. S., Gupta, D., Harsha, H. C., & Mathivanan, S. (2012). Vesiclepedia: A compendium for extracellular vesicles with continuous community annotation. *PLOS Biology*, *10*(12), e1001450. https://doi.org/10.1371/journal.pbio.1001450

Kang, J., Dietz, M. J., & Li, B. (2019). Antimicrobial peptide LL-37 is bactericidal against staphylococcus aureus biofilms. *PLoS ONE*, *14*(6), e0216676. https://doi.org/10.1371/journal.pone.0216676

Kari, O. K., Ndika, J., Parkkila, P., Louna, A., Lajunen, T., Puustinen, A., Viitala, T., Alenius, H., & Urtti, A. (2020). *In situ* analysis of liposome hard and soft protein corona structure and composition in a single label-free workflow. *Nanoscale*, *12*(3), 1728–1741. https://doi.org/10.1039/C9NR08186K

Keerthikumar, S., Chisanga, D., Ariyaratne, D., Al Saffar, H., Anand, S., Zhao, K., Samuel, M., Pathan, M., Jois, M., Chilamkurti, N., Gangoda, L., & Mathivanan, S. (2016). ExoCarta: A web-based compendium of exosomal cargo. *Journal of Molecular Biology, Computation Resources for Molecular Biology*, *428*(4), 688–692. https://doi.org/10.1016/j.jmb.2015.09.019

Killingsworth, B., Welsh, J. A., & Jones, J. C. (2021). EV translational horizons as viewed across the complex landscape of liquid biopsies. *Frontiers in Cell and Developmental Biology*, *9*(September), 556837. https://doi.org/10.3389/fcell.2021.556837

Kitka, D., Mihály, J., Fraikin, J.-L., Beke-Somfai, T., & Varga, Z. (2019). Detection and phenotyping of extracellular vesicles by size exclusion chromatography coupled with on-line fluorescence detection. *Scientific Reports*, *9*(1), 19868. https://doi.org/10.1038/s41598-019-56375-1

Ko, S. Y., & Naora, H. (2020). Extracellular vesicle membrane-associated proteins: emerging roles in tumor angiogenesis and anti-angiogenesis therapy resistance. *International Journal of Molecular Sciences*, *21*(15), 5418. https://doi.org/10.3390/ijms21155418

Li, X., Li, Y., Han, H., Miller, D. W., & Wang, G. (2006). Solution structures of human LL-37 fragments and NMR-based identification of a minimal membrane-targeting antimicrobial and anticancer region. *Journal of the American Chemical Society*, *128*(17), 5776–5785. https://doi.org/10.1021/ja0584875

Majewska, M., Zamlynny, V., Pieta, I. S., Nowakowski, R., & Pieta, P. (2021). Interaction of LL-37 human cathelicidin peptide with a model microbial-like lipid membrane. *Bioelectrochemistry*, *141*(October), 107842. https://doi.org/10.1016/j.bioelechem.2021.107842

Mangoni, M. L., Luca, V., & Mcdermott, A. M. (2015). Fighting microbial infections: A lesson from amphibian skin-derived esculentin-1 peptides. *Peptides*, *71*(September), 286–295. https://doi.org/10.1016/j.peptides.2015.04.018

Matsuhashi, S., Manirujjaman, M., Hamajima, H., & Ozaki, I. (2019). Control mechanisms of the tumor suppressor PDCD4: Expression and functions. *International Journal of Molecular Sciences*, *20*(9), 2304. https://doi.org/10.3390/ijms20092304

Milani, A., Benedusi, M., Aquila, M., & Rispoli, G. (2009). Pore forming properties of cecropin-melittin hybrid peptide in a natural membrane. *Molecules (Basel, Switzerland)*, *14*(12), 5179–5188. https://doi.org/10.3390/molecules14125179

Mishra, B., & Wang, G. (2017). Titanium surfaces immobilized with the major antimicrobial fragment FK-16 of human cathelicidin LL-37 are potent against multiple antibiotic-resistant bacteria. *Biofouling*, *33*(7), 544–555. https://doi.org/10.1080/08927014.2017.1332186

Narauskaitė, D., Vydmantaitė, G., Rusteikaitė, J., Sampath, R., Rudaitytė, A., Stašytė, G., Aparicio Calvente, M. I., & Jekabsone, A. (2021). Extracellular Vesicles in Skin Wound Healing. *Pharmaceuticals*, *14*(8), 811. https://doi.org/10.3390/ph14080811

Nasseri, S., & Sharifi, M. (2022). Therapeutic potential of antimicrobial peptides for wound healing. *International Journal of Peptide Research and Therapeutics*, *28*(1), 38. https://doi.org/10.1007/s10989-021-10350-5

Nayab, S., Aslam, M. A., Rahman, S. U., Sindhu, Z. U. D., Sajid, S., Zafar, N., Razaq, M., Kanwar, R., & Amanullah (2022). A review of antimicrobial peptides: Its function, mode of action and therapeutic potential. *International Journal of Peptide Research and Therapeutics*, *28*(1), 46. https://doi.org/10.1007/s10989-021-10325-6

Németh, A., Orgovan, N., Sódar, B. W., Osteikoetxea, X., Pálóczi, K., Szabó-Taylor, K. É., Vukman, K. V., Kittel, Á., Turiák, L., Wiener, Z., Tóth, S., Drahos, L., Vékey, K., Horvath, R., & Buzás, E. I. (2017). Antibiotic-induced release of small extracellular vesicles (exosomes) with surface-associated DNA. *Scientific Reports*, *7*(1), 8202. https://doi.org/10.1038/s41598-017-08392-1

Nguyen, V. H., & Lee, B.-J. (2017). Protein corona: A new approach for nanomedicine design. *International Journal of Nanomedicine*, *12*(April), 3137–3151. https://doi.org/10.2147/IJN.S129300

Nordén, B., Rodger, A., & Dafforn, T. (2010). Linear Dichroism and Circular Dichroism. https://pubs.rsc.org/en/content/ebook/978-1-84755-902-9

Palviainen, M., Saraswat, M., Varga, Z., Kitka, D., Neuvonen, M., Puhka, M., Joenväärä, S., Renkonen, R., Nieuwland, R., Takatalo, M., & Siljander, P. R. M. (2020). Extracellular vesicles from human plasma and serum are carriers of extravesicular cargo—Implications for biomarker discovery. *PLoS ONE*, *15*(8), e0236439. https://doi.org/10.1371/journal.pone.0236439

Pathan, M., Fonseka, P., Chitti, S. V., Kang, T., Sanwlani, R., Van Deun, J., Hendrix, A., & Mathivanan, S. (2019). Vesiclepedia 2019: A compendium of RNA, proteins, lipids and metabolites in extracellular vesicles. *Nucleic Acids Research*, *47*(D1), D516–D519. https://doi.org/10.1093/nar/gky1029

Pathan, M., Keerthikumar, S., Ang, C.-S., Gangoda, L., Quek, C. Y. J., Williamson, N. A., Mouradov, D., Sieber, O. M., Simpson, R. J., Salim, A., Bacic, A., Hill, A. F., Stroud, D. A., Ryan, M. T., Agbinya, J. I., Mariadason, J. M., Burgess, A. W., & Mathivanan, S. (2015). FunRich: An open access standalone functional enrichment and interaction network analysis tool. *Proteomics*, *15*(15), 2597–2601. https://doi.org/10.1002/pmic.201400515

Pathan, M., Keerthikumar, S., Chisanga, D., Alessandro, R., Ang, C. -S., Askenase, P., Batagov, A. O., Benito-Martin, A., Camussi, G., Clayton, A., Collino, F., Di Vizio, D., Falcon-Perez, J. M., Fonseca, P., Fonseka, P., Fontana, S., Gho, Y. S., Hendrix, A., Hoen, E. N.-T., & Mathivanan, S. (2017). A novel community driven software for functional enrichment analysis of extracellular vesicles data. *Journal of Extracellular Vesicles*, *6*(1), 1321455. https://doi.org/10.1080/20013078.2017.1321455

Pham, T. C., Jayasinghe, M. K., Pham, T. T., Yang, Y., Wei, L., Usman, W. M., Chen, H., Pirisinu, M., Gong, J., Kim, S., Peng, B., Wang, W., Chan, C., Ma, V., Nguyen, N. T. H., Kappei, D., Nguyen, X. -H., Cho, W. C., Shi, J., & Le, M. T. N. (2021). Covalent conjugation of extracellular vesicles with peptides and nanobodies for targeted therapeutic delivery. *Journal of Extracellular Vesicles*, *10*(4), e12057. https://doi.org/10.1002/jev2.12057

Pirtskhalava, M., Amstrong, A. A., Grigolava, M., Chubinidze, M., Alimbarashvili, E., Vishnepolsky, B., Gabrielian, A., Rosenthal, A., Hurt, D. E., & Tartakovsky, M. (2021). DBAASP v3: Database of antimicrobial/cytotoxic activity and structure of peptides as a resource for development of new therapeutics. *Nucleic Acids Research*, *49*(D1), D288–D297. https://doi.org/10.1093/nar/gkaa991

Pistolesi, S., Pogni, R., & Feix, J. B. (2007). Membrane Insertion and Bilayer Perturbation by Antimicrobial Peptide CM15. *Biophysical Journal*, *93*(5), 1651–1660. https://doi.org/10.1529/biophysj.107.104034

Prudent, M., Delobel, J., Hübner, A., Benay, C., Lion, N., & Tissot, J. -D. (2018). Proteomics of stored red blood cell membrane and storage-induced microvesicles reveals the association of flotillin-2 with band 3 complexes. *Frontiers in Physiology*, *9*, 421. https://www.frontiersin.org/article/10.3389/fphys.2018.00421

Quemé-Peña, M., Juhász, T., Kohut, G., Ricci, M., Singh, P., Szigyártó, I. C., Papp, Z. I., Fülöp, L., & Beke-Somfai, T. (2021). Membrane association modes of natural anticancer peptides: Mechanistic details on helicity, orientation, and surface coverage. *International Journal of Molecular Sciences*, *22*(16), 8613. https://doi.org/10.3390/ijms22168613

Rodger, A., Rajendra, J., Marrington, R., Ardhammar, M., Nordén, B., Hirst, J. D., Gilbert, A. T. B., Dafforn, T. R., Halsall, D. J., Woolhead, C. A., Robinson, C., Pinheiro, T. J. T., Kazlauskaite, J., Seymour, M., Perez, N., & Hannon, M. J. (2002). Flow oriented linear dichroism to probe protein orientation in membrane environments. *Physical Chemistry Chemical Physics*, *4*(16), 4051–4057. https://doi.org/10.1039/B205080N

Sakulkhu, U., Maurizi, L., Mahmoudi, M., Motazacker, M., Vries, M., Gramoun, A., Ollivier Beuzelin, M. -G., Vallée, J. -P., Rezaee, F., & Hofmann, H. (2014). Ex situ evaluation of the composition of protein corona of intravenously injected superparamagnetic nanoparticles in rats. *Nanoscale*, *6*(19), 11439–11450. https://doi.org/10.1039/C4NR02793K

Sartorio, M. G., Pardue, E. J., Feldman, M. F., & Haurat, M. F (2021). Bacterial outer membrane vesicles: From discovery to applications. *Annual Review of Microbiology*, *75*(October), 609–630. https://doi.org/10.1146/annurev-micro-052821-031444

Singh, P., Szigyártó, I. C., Ricci, M., Zsila, F., Juhász, T., Mihály, J., Bősze, S., Bulyáki, É., Kardos, J., Kitka, D., Varga, Z., & Beke-Somfai, T. (2020). Membrane active peptides remove surface adsorbed protein corona from extracellular vesicles of red blood cells. *Frontiers in Chemistry*, *8*, 703. https://doi.org/10.3389/fchem.2020.00703

Skotland, T., Sagini, K., Sandvig, K., & Llorente, A. (2020). An emerging focus on lipids in extracellular vesicles. *Advanced Drug Delivery Reviews*, *159*, 308–321. https://doi.org/10.1016/j.addr.2020.03.002

Sung, B. H., Ketova, T., Hoshino, D., Zijlstra, A., & Weaver, A. M. (2015). Directional cell movement through tissues is controlled by exosome secretion. *Nature Communications*, *6*(1), 7164. https://doi.org/10.1038/ncomms8164

Szigyártó, I. C., Deák, R., Mihály, J., Rocha, S., Zsila, F., Varga, Z., & Beke-Somfai, T. (2018). Flow alignment of extracellular vesicles: structure and orientation of membrane-associated bio-macromolecules studied with polarized light. *Chembiochem*, *19*(6), 545–551. https://doi.org/10.1002/cbic.201700378

Thangaraju, K., Neerukonda, S. N., Katneni, U., & Buehler, P. W. (2021). Extracellular vesicles from red blood cells and their evolving roles in health, coagulopathy and therapy. *International Journal of Molecular Sciences*, *22*(1), 153. https://doi.org/10.3390/ijms22010153

The UniProt Consortium. (2021). UniProt: The universal protein knowledgebase in 2021. *Nucleic Acids Research*, *49*(D1), D480–D489. https://doi.org/10.1093/nar/gkaa1100

Théry, C., Witwer, K. W., Aikawa, E., Alcaraz, M. J., Anderson, J. D., Andriantsitohaina, R., Antoniou, A., Arab, T., Archer, F., Atkin-Smith, G. K., Ayre, D. C., Bach, J. -M., Bachurski, D., Baharvand, H., Balaj, L., Baldacchino, S., Bauer, N. N., Baxter, A. A., Bebawy, M., & Zuba-Surma, E. K. (2018). Minimal information for studies of extracellular vesicles 2018 (MISEV2018): A position statement of the international society for extracellular vesicles and update of the MISEV2014 guidelines. *Journal of Extracellular Vesicles*, *7*(1), 1535750. https://doi.org/10.1080/20013078.2018.1535750

Tissot, J. -D., Canellini, G., Rubin, O., Angelillo-Scherrer, A., Delobel, J., Prudent, M., & Lion, N. (2013). Blood microvesicles: From proteomics to physiology. *Translational Proteomics*, *1*(1), 38–52. https://doi.org/10.1016/j.trprot.2013.04.004

Tóth, E. Á., Turiák, L., Visnovitz, T., Cserép, C., Mázló, A., Sódar, B. W., Försönits, A. I., Petővári, G., Sebestyén, A., Komlósi, Z., Drahos, L., Kittel, Á., Nagy, G., Bácsi, A., Dénes, Á., Gho, Y. S., Szabó-Taylor, K. É., & Buzás, E. I. (2021). Formation of a protein corona on the surface of extracellular vesicles in blood plasma. *Journal of Extracellular Vesicles*, *10*(11), e12140. https://doi.org/10.1002/jev2.12140

Tripathi, S., Wang, G., White, M., Qi, L., Taubenberger, J., & Hartshorn, K. L. (2015). Antiviral activity of the human cathelicidin, LL-37, and derived peptides on seasonal and pandemic influenza A viruses. *PLoS ONE*, *10*(4), e0124706. https://doi.org/10.1371/journal.pone.0124706

Tung, E. K.-K., Wong, B. Y.-C., Yau, T.-O., & Ng, I. O.-L. (2012). Upregulation of the Wnt co-receptor LRP6 promotes hepatocarcinogenesis and enhances cell invasion. *PLoS ONE*, *7*(5), e36565. https://doi.org/10.1371/journal.pone.0036565

Turiák, L., Misják, P., Szabó, T. G., Aradi, B., Pálóczi, K., Ozohanics, O., Drahos, L., Kittel, Á., Falus, A., Buzás, E. I., & Vékey, K. (2011). Proteomic characterization of thymocyte-derived microvesicles and apoptotic bodies in BALB/c mice. *Journal of Proteomics*, *74*(10), 2025–2033. https://doi.org/10.1016/j.jprot.2011.05.023

Turiák, L., Ozohanics, O., Marino, F., Drahos, L., & Vékey, K. (2011). Digestion protocol for small protein amounts for nano-HPLC-MS(MS) analysis. *Journal of Proteomics, Mass Spectrometry - One of the Pillars of Proteomics*, *74*(7), 942–947. https://doi.org/10.1016/j.jprot.2011.01.007

Valadi, H., Ekström, K., Bossios, A., Sjöstrand, M., Lee, J. J., & Lötvall, J. O. (2007). Exosome-mediated transfer of MRNAs and MicroRNAs Is a novel mechanism of genetic exchange between cells. *Nature Cell Biology*, *9*(6), 654–659. https://doi.org/10.1038/ncb1596

Vandamme, D., Landuyt, B., Luyten, W., & Schoofs, L. (2012). A comprehensive summary of LL-37, the factotum human cathelicidin peptide. *Cellular Immunology*, *280*(1), 22–35. https://doi.org/10.1016/j.cellimm.2012.11.009

Van Der Koog, L., Gandek, T. B., & Nagelkerke, A. (2022). Liposomes and extracellular vesicles as drug delivery systems: A comparison of composition, pharmacokinetics, and functionalization. *Advanced Healthcare Materials*, *11*(5), 2100639. https://doi.org/10.1002/adhm.202100639

Van Deun, J., Mestdagh, P., Agostinis, P., Akay, Ö., Anand, S., Anckaert, J., Martinez, Z. A., Baetens, T., Beghein, E., Bertier, L., Berx, G., Boere, J., Boukouris, S., Bremer, M., Buschmann, D., Byrd, J. B., Casert, C., Cheng, L., Cmoch, A., & Hendrix, A. (2017). EV-TRACK: Transparent reporting and centralizing knowledge in extracellular vesicle research. *Nature Methods*, *14*(3), 228–232. https://doi.org/10.1038/nmeth.4185

Verjans, E. -T., Zels, S., Luyten, W., Landuyt, B., & Schoofs, L. (2016). Molecular mechanisms of LL-37-induced receptor activation: An overview. *Peptides*, *85*(November), 16–26. https://doi.org/10.1016/j.peptides.2016.09.002

Wang, G. (2008). Structures of human host defense cathelicidin LL-37 and Its smallest antimicrobial peptide KR-12 in lipid micelles*. *Journal of Biological Chemistry*, *283*(47), 32637–32643. https://doi.org/10.1074/jbc.M805533200

Wang, C., Chen, B., He, M., & Hu, B. (2021). Composition of intracellular protein corona around nanoparticles during internalization. *ACS Nano*, *15*(2), 3108–3122. https://doi.org/10.1021/acsnano.0c09649

Wang, G., Narayana, J. L., Mishra, B., Zhang, Y., Wang, F., Wang, C., Zarena, D., Lushnikova, T., & Wang, X. (2019). Design of antimicrobial peptides: progress made with human cathelicidin LL-37. *Advances in Experimental Medicine and Biology*, *1117*, 215–240. https://doi.org/10.1007/978-981-13-3588-4_12

Wang, Y., Schlamadinger, D. E., Kim, J. E., & Mccammon, J. A (2012). Comparative molecular dynamics simulations of the antimicrobial peptide CM15 in model lipid bilayers. *Biochimica Et Biophysica Acta (BBA) - Biomembranes*, *1818*(5), 1402–1409. https://doi.org/10.1016/j.bbamem.2012.02.017

Wheeler, K. E., Chetwynd, A. J., Fahy, K. M., Hong, B. S., Tochihuitl, J. A., Foster, L. A., & Lynch, I. (2021). Environmental dimensions of the protein corona. *Nature Nanotechnology*, *16*(6), 617–629. https://doi.org/10.1038/s41565-021-00924-1

Williams, C., Pazos, R., Royo, F., González, E., Roura-Ferrer, M., Martinez, A., Gamiz, J., Reichardt, N. -C., & Falcón-Pérez, J. M. (2019). Assessing the role of surface glycans of extracellular vesicles on cellular uptake. *Scientific Reports*, *9*(1), 11920. https://doi.org/10.1038/s41598-019-48499-1

Wolf, M., Poupardin, R. W., Ebner-Peking, P., Andrade, A. C., Blöchl, C., Obermayer, A., Gomes, F. G., Vari, B., Maeding, N., Eminger, E., Binder, H. -M., Raninger, A. M., Hochmann, S., Brachtl, G., Spittler, A., Heuser, T., Ofir, R., Huber, C. G., Aberman, Z., & Strunk, D. (2022). A functional corona around extracellular vesicles enhances angiogenesis, skin regeneration and immunomodulation. *Journal of Extracellular Vesicles*, *11*(4), e12207. https://doi.org/10.1002/jev2.12207

Xu, L., Liang, Y., Xu, X., Xia, J., Wen, C., Zhang, P., & Duan, L. (2021). Blood cell-derived extracellular vesicles: Diagnostic biomarkers and smart delivery systems. *Bioengineered*, *12*(1), 7929–7940. https://doi.org/10.1080/21655979.2021.1982320

Yang, Y., Hong, Y., Cho, E., Kim, G. B., & Kim, I.-S. (2018). Extracellular vesicles as a platform for membrane-associated therapeutic protein delivery. *Journal of Extracellular Vesicles*, *7*(1), 1440131. https://doi.org/10.1080/20013078.2018.1440131

Yerneni, S. S., Solomon, T., Smith, J., & Campbell, P. G. (2022). Radioiodination of extravesicular surface constituents to study the biocorona, cell trafficking and storage stability of extracellular vesicles. *Biochimica Et Biophysica Acta (BBA) - General Subjects*, *1866*(2), 130069. https://doi.org/10.1016/j.bbagen.2021.130069

Yuan, Y., Xie, X., Jiang, Y., Wei, Z., Wang, P., Chen, F., Li, X., Sun, C., Zhao, H., Zeng, X., Jiang, L., Zhou, Y., Dan, H., Feng, M., Liu, R., Wang, Z., & Chen, Q. (2017). LRP6 is identified as a potential prognostic marker for oral squamous cell carcinoma via MALDI-IMS. *Cell Death & Disease*, *8*(9), e3035–e3035. https://doi.org/10.1038/cddis.2017.433

Zhang, H., Wu, T., Yu, W., Ruan, S., He, Q., & Gao, H. (2018). Ligand size and conformation affect the behavior of nanoparticles coated with in vitro and in vivo protein corona. *ACS Applied Materials & Interfaces*, *10*(10), 9094–9103. https://doi.org/10.1021/acsami.7b16096

Zhou, J., Wu, Z., Hu, J., Yang, D., Chen, X., Wang, Q., Liu, J., Dou, M., Peng, W., Wu, Y., Wang, W., Xie, C., Wang, M., Song, Y., Zeng, H., & Bai, C. (2020). High-throughput single-EV liquid biopsy: Rapid, simultaneous, and multiplexed detection of nucleic acids, proteins, and their combinations. *Science Advances*, *6*(47), eabc1204. https://doi.org/10.1126/sciadv.abc1204

Zsila, F., Kohut, G., & Beke-Somfai, T. (2019). Disorder-to-helix conformational conversion of the human immunomodulatory peptide LL-37 induced by anti-inflammatory drugs, food dyes and some metabolites. *International Journal of Biological Macromolecules*, *129*(May), 50–60. https://doi.org/10.1016/j.ijbiomac.2019.01.209

Zsila, F., Ricci, M., Szigyártó, I. C., Singh, P., & Beke-Somfai, T. (2021). Quorum sensing pseudomonas quinolone signal forms chiral supramolecular assemblies with the host defense peptide LL-37. *Frontiers in Molecular Biosciences*, *8*(October), 742023. https://doi.org/10.3389/fmolb.2021.742023

SUPPORTING INFORMATION

Additional supporting information can be found online in the Supporting Information section at the end of this article.

How to cite this article: Singh, P., Szigyártó, I. C., Ricci, M., Gaál, A., Peña, M. M. Q., Kitka, D., Fülöp, L., Turiák, L., Drahos, L., Varga, Z., & Beke-Somfai, T. (2023). Removal and identification of external protein corona members from RBC-derived extracellular vesicles by surface manipulating antimicrobial peptides. *Journal of Extracellular Biology*, *2*, e78. https://doi.org/10.1002/jex2.78